



Redox-Linked Structural Changes in Ribonucleotide Reductase

The MIT Faculty has made this article openly available. ***Please share*** how this access benefits you. Your story matters.

Citation	Offenbacher, A. R., I. R. Vassiliev, M. R. Seyedsayamdost, J. Stubbe, and B. A. Barry. "Redox-Linked Structural Changes in Ribonucleotide Reductase." <i>Journal of the American Chemical Society</i> 131, no. 22 (June 10, 2009): 7496-7497.
As Published	http://dx.doi.org/10.1021/ja901908j
Publisher	American Chemical Society (ACS)
Version	Author's final manuscript
Accessed	Wed Jan 27 06:46:48 EST 2016
Citable Link	http://hdl.handle.net/1721.1/82563
Terms of Use	Article is made available in accordance with the publisher's policy and may be subject to US copyright law. Please refer to the publisher's site for terms of use.
Detailed Terms	

Published in final edited form as:

J Am Chem Soc. 2009 June 10; 131(22): 7496–7497. doi:10.1021/ja901908j.

Redox-linked Structural Changes in Ribonucleotide Reductase

A. R. Offenbacher¹, I. R. Vassiliev^{1,‡}, M. R. Seyedsayamdost², J. Stubbe², and B. A. Barry^{1,*}

¹ Department of Chemistry and Biochemistry and the Petit Institute for Bioengineering and Bioscience, Georgia Institute of Technology, Atlanta, GA 30332

² Departments of Chemistry and Biology, Massachusetts Institute of Technology, Cambridge, MA 02139

Abstract

Ribonucleotide reductase (RNR) catalyzes the reduction of ribonucleotides to deoxyribonucleotides. Class I RNRs are composed of two homodimeric proteins, $\alpha 2$ and $\beta 2$. The class Ia *E. coli* $\beta 2$ contains dinuclear, antiferromagnetically coupled iron centers and one tyrosyl free radical, Y122•/ $\beta 2$. Y122• acts as a radical initiator in catalysis. Redox-linked conformational changes may accompany Y122 oxidation and provide local control of proton-coupled electron transfer reactions. To test for such redox-linked structural changes, FT-IR spectroscopy was employed in this work. Reaction-induced difference spectra, associated with the reduction of Y122• by hydroxyurea, were acquired from natural abundance, ²H₄ tyrosine, and ¹⁵N tyrosine labeled $\beta 2$ samples. Isotopic labeling led to the assignment of a 1514 cm⁻¹ band to the ν 19a ring stretching vibration of Y122 and of a 1498 cm⁻¹ band to the ν 7a CO stretching vibration of Y122•. The reaction-induced spectra also exhibited amide I bands, at 1661 and 1652 cm⁻¹. A similar set of amide I bands, with frequencies of 1675 and 1651 cm⁻¹, was observed when Y• was generated by photolysis in a pentapeptide, which matched the primary sequence surrounding Y122. This result suggests that reduction of Y122• is linked with structural changes at nearby amide bonds and that this perturbation is mediated by the primary sequence. To explain these data, we propose that a structural perturbation of the amide bond is driven by redox-linked electrostatic changes in the tyrosyl radical aromatic ring.

Ribonucleotide reductase (RNR) catalyzes the reduction of ribonucleotides to deoxyribonucleotides.^{1–3} Class I RNRs are composed of a 1:1 complex of two homodimeric proteins, $\alpha 2$ and $\beta 2$. $\alpha 2$ contains the binding site for substrates and allosteric effectors that govern turnover rate and specificity, and $\beta 2$ houses the essential diferrityrosyl radical (residue 122, Y122•) cofactor.^{1–4} Y122• acts as a radical initiator, generating a thiyl radical in $\alpha 25$, ~35 Å removed.^{6–8} Long distance proton coupled electron transfer (PCET) is facilitated by a series of amino acid radical intermediates, which serve to accelerate the reaction rate into a physiologically relevant range.^{9–15}

In this work, vibrational spectroscopy is used to show that electron transfer to and from the tyrosyl radical (Y122•) in RNR is coupled to a conformational change in the $\beta 2$ subunit. Such redox-linked conformational changes are important because they can modulate the interaction of Y122 with its hydrogen bonding partner and provide local, structural control of its PCET reactions.

*bridgette.barry@chemistry.gatech.edu.

‡Deceased, August 10, 2005

Supporting Information Available: Description of the expression/purification of the $\beta 2$ subunit, the FT-IR methods, the kinetic studies, and acknowledgments. This information is available free of charge via the Internet at <http://pubs.acs.org/>.

In previous work, high resolution magnetic resonance studies of Y122•¹⁶ were performed. Comparison with the X-ray structure of reduced $\beta 2$ suggested that a C $_{\alpha}$ -C $_{\beta}$ single bond rotation may occur when Y122 is oxidized. This single bond rotation was attributed to an electrostatic repulsion between Asp-84 and Y122• and would disconnect Y122• from the hydrogen bond network at the diiron site. A Y• conformational rearrangement has also been proposed to occur with Y oxidation in pentapeptides and tyrosinate at 85 K.¹⁷

To identify redox-linked structural changes associated with electron transfer reactions in $\beta 2$, we have performed FT-IR spectroscopy on the purified *E. coli* subunit in ²H₂O buffer (Supplemental information, Figs. S1 and S2). FT-IR spectroscopy has emerged as a powerful tool in elucidating enzyme mechanisms {reviewed in ref 18}. This approach has been used to study redox-active tyrosines in other proteins, such as photosystem II¹⁹ and cytochrome *c* oxidase.²⁰

The reaction-induced difference spectrum, associated with the reduction of Y122•, is presented in Figs. 1A and 2A. These data were acquired by one electron reduction of Y122• with hydroxyurea^{21–24} over 10 min. Based on the rate constant in ²H₂O (Figs. S3 and S4), an estimated ~60% of Y122• is reduced during the 10 min FT-IR measurement.

In the difference spectrum shown in Fig. 1A, unique bands of tyrosyl radical, Y122•, will be positive features; unique bands of Y122 will be negative features. Using model compounds and DFT calculations, it has been shown that oxidation of tyrosine leads to an upshift of the CO stretching vibration to 1516 cm⁻¹ ($\nu 7a$) and to perturbations of the aromatic ring stretching frequencies, at ~1600 ($\nu 8a$) and ~1500 ($\nu 19a$) cm⁻¹ {Figs. 1A and 2A) and see ref 25 and refs therein}. Oxidation of the tyrosine aromatic side chain in peptides and in tyrosinate at pH 11 gave similar results for the CO and $\nu 19a$ ring stretching modes {Fig. 1D and E and refs 17,26}. Previous Raman studies of the *E. coli* and mouse $\beta 2$ subunits have attributed bands at 1498²⁷ and 1515²⁸ cm⁻¹, respectively, to the CO vibration.

To identify Y122•/Y122 contributions to the natural abundance spectrum (Figs. 1A and 2A), the $\beta 2$ subunit was labeled with the ²H₄-tyrosine isotopomer (Figs. 1B and 2B). ²H₄ tyrosine labeling resulted in a downshift of a negative band at 1514 cm⁻¹ to 1432 cm⁻¹ (Figs. 2A and B). This band was not observed in a negative Met $\beta 2$ control (Fig. 1F) or in a negative control, in which the $\beta 2$ subunit was mixed with buffer instead of hydroxyurea (Fig. 1G). Based on previous model compound studies and DFT calculations²⁵, we assign this band to a ring stretching vibration ($\nu 19a$) of Y122. From DFT calculations, the expected isotope-induced downshift is 80 cm⁻¹.²⁵

²H₄ labeling also resulted in a downshift of a positive band at 1498 cm⁻¹ to 1480 cm⁻¹ (Figs. 2A and B). This band was not observed in the negative controls (Figs. 1F or G) and is assigned to the CO stretching vibration ($\nu 7a$) of Y122•. From DFT calculations, the expected isotope-induced downshift is ~20 cm⁻¹.²⁵ The assignment of the 1498 cm⁻¹ band is in agreement with previous Raman studies.²⁷

These data establish that the CO vibrational band of Y122• is downshifted ~20 cm⁻¹ from its frequency in Y• model compounds,^{17,25} where it is observed as a positive band at 1516 cm⁻¹ (Fig. 1D and E). The symmetric ring stretching mode, $\nu 8a$, at negative 1605 cm⁻¹ (Fig. 1E) was not observed when Y• is generated in the pentapeptide (Fig. 1D) or in $\beta 2$ (Fig. 1A).

In addition to bands associated with tyrosine oxidation, the reaction-induced spectrum in Fig. 1A reveals coupled, oxidation-induced effects on the protein environment. For example, Fig. 1A exhibits a negative band at 1661 cm⁻¹ and a positive band at 1652 cm⁻¹. This is a

spectral region characteristic of amide I C=O vibrational bands.²⁹ These data suggest that Y122• reduction is coupled with a structural change in the $\beta 2$ subunit.

As a first step in interpretation of the amide I spectral contributions, we studied a pentapeptide, RSYTH, matching the sequence containing Y122 in the $\beta 2$ subunit.¹⁷ The pentapeptide spectrum in $^2\text{H}_2\text{O}$ buffer (Fig. 1D) exhibited several bands in the amide I region, at 1675 and 1651 cm^{-1} , which were not observed when tyrosyl radical was generated in a powder tyrosinate sample (Fig. 1E).¹⁷ This result suggests that electron transfer reactions are linked with a structural change in one or more peptide bonds in the pentapeptide and in the $\beta 2$ sample. Because the pentapeptide is expected to have no defined structure in solution, the primary sequence must mediate this redox-linked interaction. We propose that this conformational change occurs at adjacent peptide bonds to Y122•.

^{15}N -labeling of tyrosine in $\beta 2$ was employed (Fig. 1C and 2C) to test if the structural perturbation occurs at the S121-Y122 amide bond. The effect of ^{15}N labeling is expected to be detectable {for example, see ref 30 }, because the amide I normal mode involves nitrogen displacement.²⁹ However, ^{15}N labeling had no significant effect on the reaction-induced spectrum (Figs. 2A and C). This result is consistent with the conclusion that the redox-linked structural change does not perturb the Ser-Tyr amide linkage, but other amide bonds near Y122.

We hypothesize that the structural perturbation of the amide bond in the $\beta 2$ and the pentapeptide samples is driven by an electrostatic change. Electrostatic maps predict a change in aromatic ring charge distribution.³¹ An oxidation-induced change in charge distribution will lead to alterations in the C-N bond ionic character, planarity, and force constant through a Stark effect. This interpretation is congruent with recent ESEEM studies of pentapeptide samples, which have shown sequence-dependent changes in nuclear quadrupole interactions in tyrosyl radicals.³²

Redox-linked structural changes at Y122/Y122• may partially control PCET reactions during the RNR reaction cycle.^{5,16} These conformational alterations are likely to cause changes in Y122 interactions with its hydrogen bonding partner.¹⁶ Therefore, these structural changes may play a role in regulation of Y122 midpoint potential and its reversible protonation/deprotonation reactions. This work provides spectroscopic evidence for dynamic structural changes in RNR.

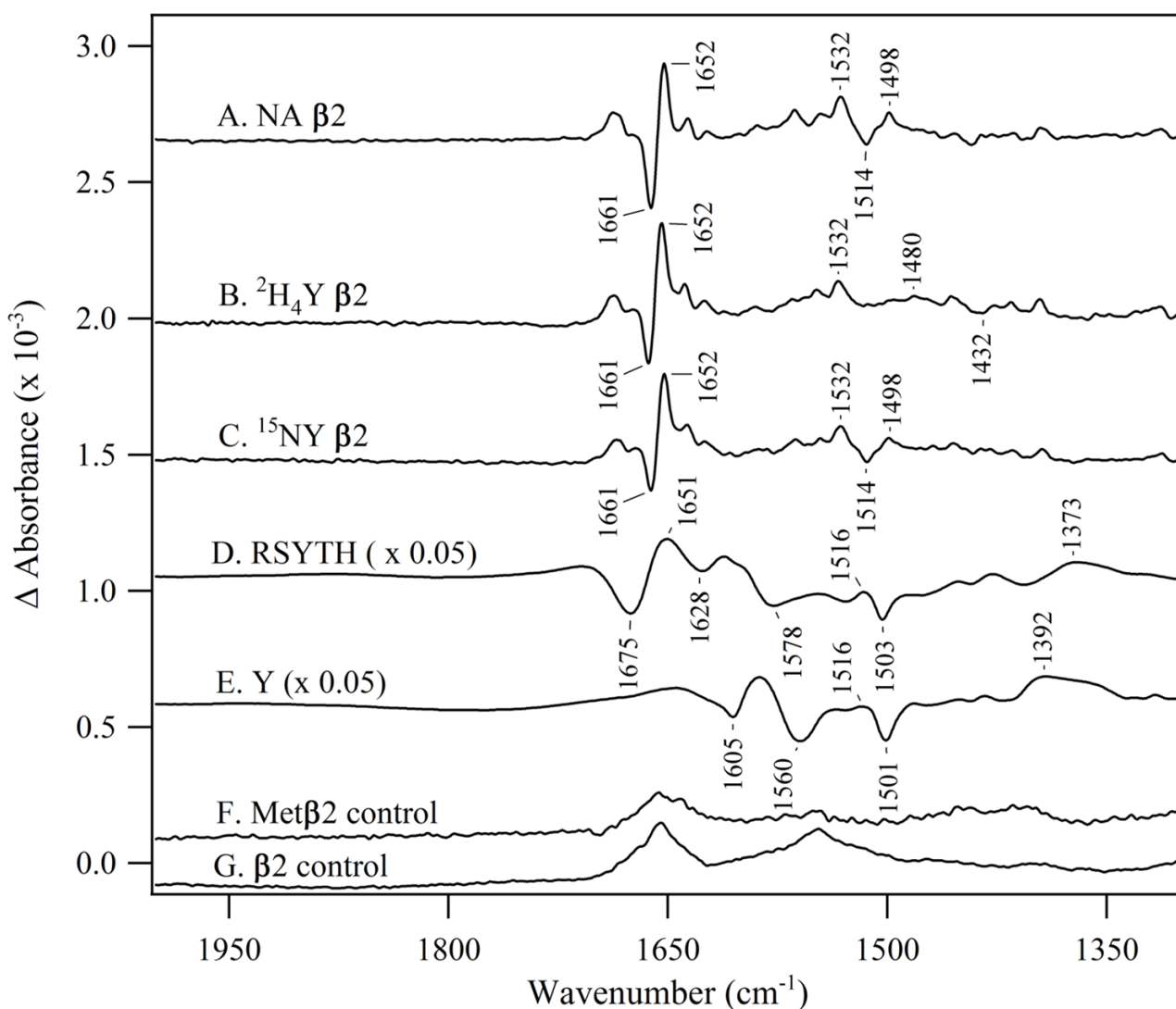
Supplementary Material

Refer to Web version on PubMed Central for supplementary material.

References

1. Sjöberg BM, Reichard P, Gräslund A, Ehrenberg A. *J Biol Chem* 1978;253:6863–6865. [PubMed: 211133]
2. Stubbe J. *J Biol Chem* 1990;265:5329–5332. [PubMed: 2180924]
3. Nordlund P, Sjöberg BM, Eklund H. *Nature* 1990;345:593–598. [PubMed: 2190093]
4. Nordlund P, Eklund H. *J Mol Biol* 1993;232:123–164. [PubMed: 8331655]
5. Stubbe J, van der Donk WA. *Chem Rev* 1998;98:705–762. [PubMed: 11848913]
6. Uhlin U, Eklund H. *Nature* 1994;370:533–539. [PubMed: 8052308]
7. Bennati M, Robblee JH, Mugnaini V, Stubbe J, Freed JH, Borbat P. *J Am Chem Soc* 2005;127:15014–15015. [PubMed: 16248626]
8. Uppsten M, Färnegårdh M, Domkin V, Uhlin U. *J Mol Biol* 2006;359:365–377. [PubMed: 16631785]

9. Rova U, Goodtzova K, Ingemarson R, Behravan G, Gräslund A, Thelander L. *Biochemistry* 1995;34:4267–4275. [PubMed: 7703240]
10. Ekberg M, Sahlin M, Eriksson M, Sjöberg BM. *J Biol Chem* 1996;271:20655–20659. [PubMed: 8702814]
11. Ekberg M, Pötsch S, Sandin E, Thunnissen M, Nordlund P, Sahlin M, Sjöberg BM. *J Biol Chem* 1998;273:21003–21008. [PubMed: 9694851]
12. Yee CS, Chang MCY, Ge J, Nocera DG, Stubbe J. *J Am Chem Soc* 2003;125:10506–10507. [PubMed: 12940718]
13. Seyedsayamdost MR, Stubbe J. *J Am Chem Soc* 2006;128:2522–2523. [PubMed: 16492021]
14. Seyedsayamdost MR, Yee CS, Reece SY, Nocera DG, Stubbe J. *J Am Chem Soc* 2006;128:1562–1568. [PubMed: 16448127]
15. Seyedsayamdost MR, Xie J, Chan CTY, Schultz PG, Stubbe J. *J Am Chem Soc* 2007;129:15060–15071. [PubMed: 17990884]
16. Högbom M, Galander M, Andersson M, Kolberg M, Hofbauer W, Lassmann G, Nordlund P, Lendzian F. *Proc Natl Acad Sci USA* 2003;100:3209–3214. [PubMed: 12624184]
17. Vassiliev IR, Offenbacher AR, Barry BA. *J Phys Chem B* 2005;109:23077–23085. [PubMed: 16854006]
18. Kötting C, Gerwert K. *ChemPhysChem* 2005;6:881–888. [PubMed: 15884070]
19. Kim S, Liang J, Barry BA. *Proc Natl Acad Sci USA* 1997;94:14406–14411. [PubMed: 9405625]
20. Iwaki M, Puustinen A, Wikström M, Rich PR. *Biochemistry* 2006;45:10873–10885. [PubMed: 16953573]
21. Ehrenberg A, Reichard P. *J Biol Chem* 1972;247:3485–3488. [PubMed: 4337857]
22. Larsen IK, Sjöberg BM, Thelander L. *Eur J Biochem* 1982;125:75–81. [PubMed: 7049700]
23. Karlsson M, Sahlin M, Sjöberg BM. *J Biol Chem* 1992;267:12622–12626. [PubMed: 1618767]
24. Han JY, Gräslund A, Thelander L, Sykes AG. *J Biol Inorg Chem* 1997;2:287–294.
25. Range K, Ayala I, York D, Barry BA. *J Phys Chem B* 2006;110:10970–10981. [PubMed: 16771350]
26. Ayala I, Range K, York D, Barry BA. *J Am Chem Soc* 2002;124:5496–5505. [PubMed: 11996592]
27. Backes G, Sahlin M, Sjöberg BM, Loehr TM, Sanders-Loehr J. *Biochemistry* 1989;28:1923–1929. [PubMed: 2655700]
28. Hanson MA, Schmidt PP, Strand KR, Gräslund A, Solomon EI, Andersson KK. *J Am Chem Soc* 1999;121:6755–6756.
29. Krimm, S.; Bandekar, J. *Advances in Protein Chemistry*. Anfinsen, CB.; Edsall, JT.; Richards, FM., editors. Vol. 38. Academic Press; New York: 1986. p. 181–364.
30. Kim S, Barry BA. *Biophys J* 1998;74:2588–2600. [PubMed: 9591683]
31. Sibert R, Josowicz M, Porcelli F, Veglia G, Range K, Barry BA. *J Am Chem Soc* 2007;129:4393–4400. [PubMed: 17362010]
32. McCracken J, Vassiliev IR, Yang EC, Range K, Barry BA. *J Phys Chem B* 2007;111:6586–6592. [PubMed: 17518496]

**Figure 1.**

Reaction-induced FT-IR spectra, monitoring redox-linked structural changes induced by Y122• reduction with 50 mM hydroxyurea. Spectra (A-C, F and G) were acquired at 20°C in $^2\text{H}_2\text{O}$ buffer. In (A), the (250 μM) $\beta 2$ sample was natural abundance, in (B) $^2\text{H}_4$ -tyrosine labeled, and in (C) ^{15}N -tyrosine labeled. In (D) and (E), Y• was generated using 266 nm photolysis at 80 K in the RSTYH peptide (D) or in tyrosinate (E) at p ^2H 11. (F) is a (250 μM) Met $\beta 2$ control difference spectrum, which lacks Y122•, but was mixed with hydroxyurea. (G) is a (250 μM) $\beta 2$ control difference spectrum, in which $\beta 2$ was mixed with buffer, instead of hydroxyurea. The difference spectra were constructed: Y•-minus-Y. The spectra are averages from 8 (A), 6 (B), 8 (C), 5 (D), 3 (E), 6 (F), and 11 (G) samples.

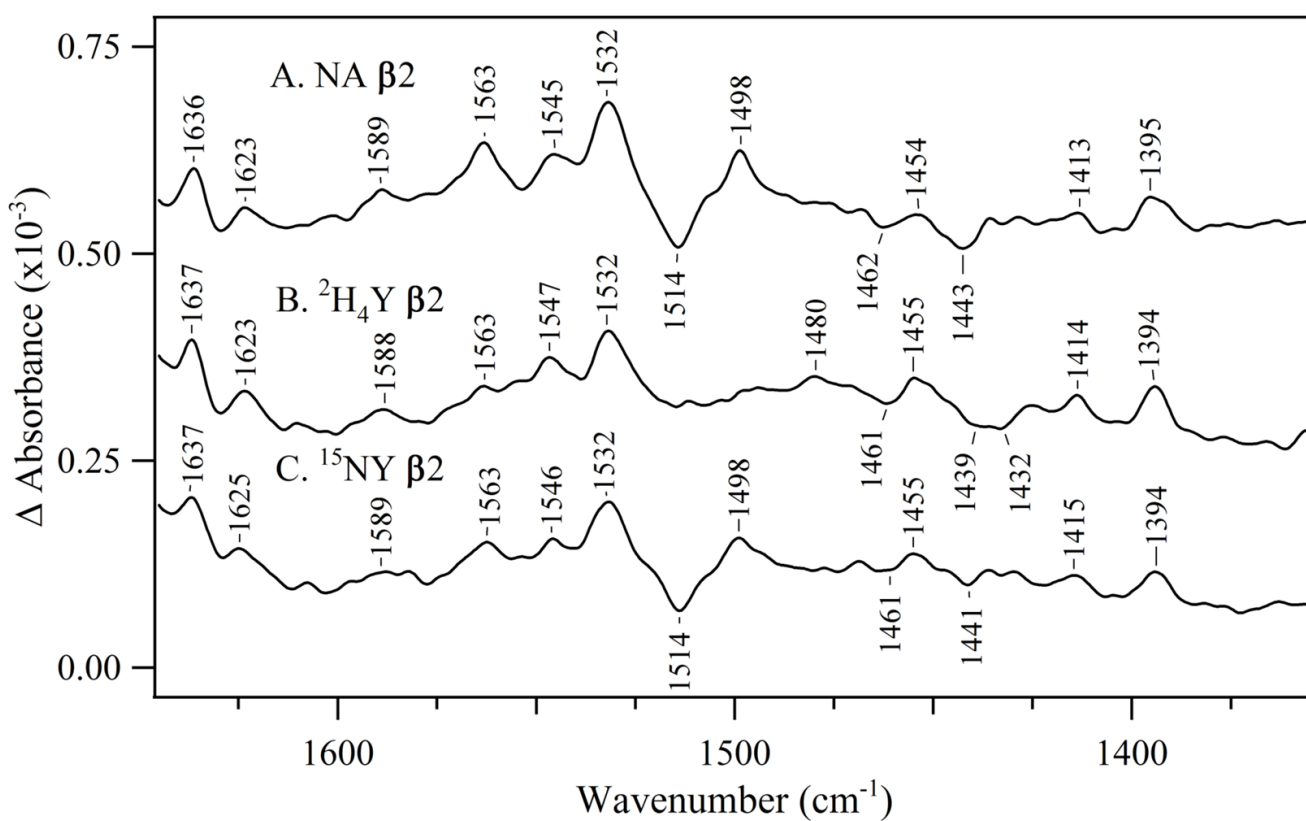


Figure 2.

The 1700-1300 cm^{-1} region of the reaction-induced FT-IR spectrum, monitoring redox-linked structural changes induced by Y122• reduction with 50 mM hydroxyurea. Spectra 2A, B and C are expanded and repeated from Fig. 1A, B and C, respectively.